International Journal of GEOMATE, March., 2024 Vol.26, Issue 115, pp.100-107
ISSN: 2186-2982 (P), 2186-2990 (O), Japan, DOI: https://doi.org/10.21660/2024.115.g13401
Geotechnique, Construction Materials and Environment

INVESTIGATION OF THE COLLAPSE OF THE CINCIN LAMA BRIDGE WITH CONSIDERATION OF FATIGUE DAMAGE

*Made Suarjana[1], and Anastasia Mani' Sarungallo[2]

[1]Faculty of Civil and Environmental Engineering, Institut Teknologi Bandung, Indonesia;
[2]Directorate General of Highways, Ministry of Public Works and Housing, Indonesia

*Corresponding Author, Received: 00 Oct. 2018, Revised: 00 Nov. 2023, Accepted: 00 Dec. 2023

ABSTRACT: The Cincin Lama bridge is a crucial component of a major road in Java Island, Indonesia. It comprises six spans of the Callender Hamilton-type truss bridge, with each span measuring 50 meters. Tragically, one of its six spans collapsed during operation on April 17th, 2018. To understand the cause behind this incident and extract valuable lessons from it, an investigation utilizing finite element analysis was initiated. The primary objective of this investigation was to pinpoint the root cause that precipitated the collapse of the bridge. To achieve this critical goal, the investigation commenced with a thorough examination of the site investigation reports, coupled with an assessment of the bridge's adherence to the Indonesian design code applicable during its construction. Subsequently, the bridge underwent analysis based on the most recent Indonesian codes, taking into account the estimated ultimate load experienced at the time of the accident. To consider the possibility of pre-existing defects that may have contributed to the collapse, a fatigue analysis was also conducted. To ensure a precise estimation of the traffic load, weight in motion (WIM) data was utilized in the fatigue analysis. Through this detailed examination, it was revealed that the collapse was most likely triggered by a combination of an overloaded truckload and accumulated fatigue damage prior to the accident. The knowledge gained from this investigation will undoubtedly contribute to the improvement of safety measures and engineering practices in the construction of bridges, ensuring a more secure infrastructure for Indonesia's transportation network.

Keywords: Collapse investigation, Cincin Lama Bridge, Fatigue analysis, WIM, Truss bridge

1. INTRODUCTION

The collapse of the Cincin Lama Bridge on April 17, 2018, was sudden and one of the tragic collapses to occur on Indonesia's transportation network. The bridge connecting Lamongan Regency with Tuban Regency in East Java province is part of the main transportation network on the island of Java. The bridge, which crosses over the Bengawan Solo River, is part of a route that is heavily used by large vehicles.

The Cincin Lama Bridge is a Callender Hamilton-type steel truss bridge built in 1977, making it 41 years old at the time of its collapse. The bridge consists of six spans, with five spans made of steel trusses and one span made of concrete girders. The fourth span from the East direction collapsed. Fig.1 depicts a sketch of the Cincin Lama Bridge showing the location of the collapsed span. Fig.2 shows a photo of the collapsed span. From field observations, as also clearly shown in Fig.2, the collapse is evident in the vicinity of one of the supports. At the time of the collapse, three heavy trucks and a motorcycle were crossing the bridge, and these vehicles fell along with the bridge.

Bridges play a crucial role as an essential infrastructure supporting the social and economic development of a country. However, it is unfortunate that bridge failures are frequently being reported [1,2,3,4,5,6,7]. One of the frequent causes of bridge collapse is vehicle overloading. Vehicle overloading can significantly shorten the fatigue life of a bridge and even lead to its immediate collapse [2,8,9,10].

Despite the ductility of steel material, the collapse of a steel bridge can happen abruptly, without any warning, as exemplified by the I-35W Mississippi Bridge (2007) in the USA, the Kartanegara Bridge (2011), and the Palu IV Bridge (2018), both in Indonesia.

The collapse of the 40-year-old I-35W steel deck truss bridge over the Mississippi River in Minneapolis, United States, was initiated by the failure of a single gusset plate, subsequently leading to the progressive collapse of the main framework [11,12]. Astaneh-Asl [11] also emphasized that the bridge lacks redundancy and is a determinate system, making it susceptible to progressive collapse if a crucial component fails.

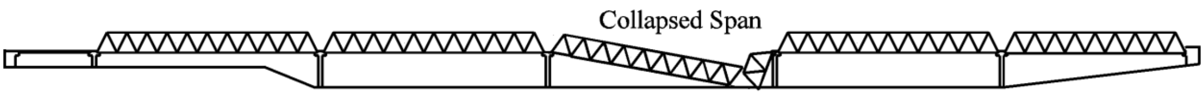

Fig.1 Sketch of The Cincin Lama Bridge

The collapse of the Kutai-Kartanegara Bridge was triggered by jacking force applied during maintenance work. This force potentially led to overstress on the cable hanger connections, which have flaws in design, material selection, and maintenance [13]. Imran [14] reported that the collapse of the Palu IV Bridge was caused by an extreme load resulting from a nearby earthquake, which was not considered during the design process.

In this study, an evaluation was conducted to investigate the possible causes of the collapse of the Cincin Lama Bridge. The evaluation was carried out by analyzing the bridge's strength in withstanding extreme loads based on three criteria: compliance with the design code at the time of bridge construction, compliance with the current design code in Indonesia, and based on the estimated actual load at the time before the collapse occurred. Fatigue analysis was also performed to examine the possibility of the bridge experiencing fatigue damage prior to the load that led to its collapse. Fatigue analysis utilized the Weigh-in-Motion (WIM) data that had been measured for the road section served by the bridge.

Fig.2 Photo of the collapsed span (documentation of Directorate for Eng. Affairs of Roads and Bridges, Ministry of Public Work and Housing, Indonesia)

2. RESEARCH SIGNIFICANT

In Indonesia, there are still many Callender Hamilton bridges of a similar age that are still in operation on busy traffic routes and are frequently crossed by heavy-loaded vehicles. It is crucial to understand why the collapse of the Cincin Lama Bridge occurred to take preventive measures and avoid the recurrence of similar incidents. Furthermore, the utilization of Weigh-in-Motion (WIM) data is anticipated to yield substantial enhancements in fatigue analyses. This is attributed to the utilization of improved and more realistic traffic load data.

3. BRIDGE DATA AND SURVEY RESULTS

Bridge data was collected from the archives of the Indonesian Ministry of Public Works [15,16]. In addition, a field survey was conducted to verify the bridge data and assess the bridge's condition. The bridge consists of six spans, including five spans of steel truss and one concrete girder. Fig.1 illustrates the side view of the bridge and Table 1 lists the main data of the bridge. To perform the strength check, we assess both the bridge load based on Indonesian codes and the actual load during the collapse incident. Additionally, we use weigh-in-motion (WIM) measurements to estimate the fatigue load.

3.1 Main Truss

The main structure of the Cincin Lama Bridge is a Callender Hamilton-type bridge, which essentially is a Warren truss framework. Each truss member is constructed using two compound sections joined together with batten plates in three locations. Each compound section is formed by assembling two, three, or four L150x150x11.7 angle sections using bolts. Fig.3 illustrates half of the span of a typical steel truss framework. The numbers depicted in the figure indicate the number of angle sections combined to form the member section. For instance, Fig.4 showcases a 4-3 section. Truss joints are created through bolt connections, as illustrated in Fig. 5, which provides a detailed example of this connection.

Table 1 Cincin Lama Bridge main data

Properties	Value
Total bridge length	259 m
Length of collapsed span	50.29 m
Total bridge width	9.5 m
Road width	7.0 m
Pedestrian width	2 x 1 m
Number of steel truss spans	5
Number of concrete girder span	1
Pedestrian additional thickness	175 mm
Concrete slab thickness	200 mm
Asphalt thickness	50 mm

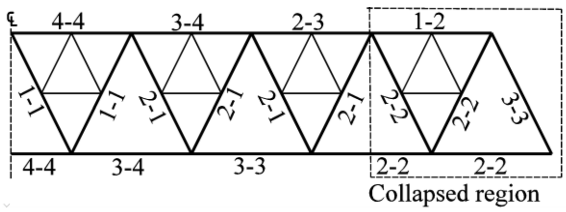

Fig.3 Half span of the typical steel truss

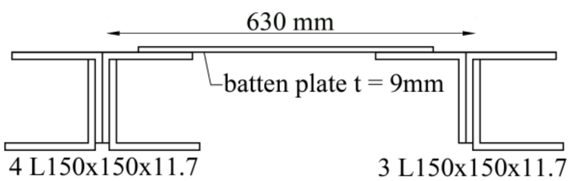

Fig.4 Built-in 4-3 section

Fig.5 An example of the connection detail

3.2 Material Type and Properties

The material types and properties of the Cincin Lama Bridge are shown in Table 2.

Table 2 Structural material type and properties

Element	Mat. type	Yield stress
Main chord	BS 4360 Gr. 55C	430 MPa
Brace	BS 4360 Gr. 43A	250 MPa
Trans. girder	SS400	215 MPa
Stringer	SS400	215 MPa
Gusset plate	BS 4360 Gr. 50B	350 MPa

3.3 Field Survey of The Bridge

The size and configuration of the bridge elements were verified through field surveys on the intact bridge spans. In general, the drawings and data correspond to the field conditions. The bridges are generally in good condition and show no visible corrosion or evident signs of wear. The discovery of welds on the gusset plate, presumably intended to repair the detected cracks, is somewhat alarming.

3.4 Data on Trucks Overloading the Bridge

Three trucks fell with the bridge: one of the 2-axle type and the other two of the 3-axle type. To determine the dimensions and weight of these trucks, we relied on data from standard trucks commonly used in Indonesia. The load weight was estimated by considering the volume capacity of trucks carrying sand for the 2-axle truck and cement smelters for the 3-axle trucks. The precise load estimates utilized in the analysis can be found in Table 3.

Table 3 Estimated actual load

Truck	Axle distance (m)		Axle Load (kN)		
	1 – II	II – III	I	II	III
2 axles	4.33	-	12	23	0
3 axles	4.03	1.3	11	18	18

3.5 Fatigue Load

The load used for fatigue evaluation is derived from the weigh-in-motion (WIM) measurements conducted on the Tuban-Gresik Road section in East Java, Indonesia. This road segment serves as a crucial artery that spans the Cincin Lama Bridge. WIM has been used for fatigue analysis of bridges for more accurate traffic load data [17,18,19,20,21].

According to SNI 1725-2016 [22] and AASHTO LRFD 2012 [23] codes, the vehicle classes considered from the WIM data for fatigue are only trucks and buses. The available WIM data consists of measurements taken over a period of five days, recording a total of 43,361 vehicles, of which 27,922 were trucks or buses. The average daily traffic for trucks or buses amounts to 5,584 units. The distribution of truck or bus counts based on their weights is also provided. These measurement results are considered as annual average daily traffic (AADT) for the measurement year. The AADT for years other than the measurement year is estimated using Eq. (1), which is adopted from [24].

$$AADT_{Future} = AADT_{current} * (1 + AACR)^{n} \quad (1)$$

where $AADT_{Future}$ is the annual average daily traffic for the forecaster year (vehicle/day), $AADT_{Current}$ is the annual average daily traffic for the current year, $AACR$ is the annual average change rate, taken as 4.8% and n is the number of forecasted years.

Equation (1) was employed to project the vehicle count for the entire service life of the bridge, which spans 41 years. The total number of vehicles was then calculated for 41 years and averaged to determine the annual vehicle count. The processed WIM data, indicating the average number of vehicles per year over the bridge's service life, is presented in Table 4.

Table 4 Number of vehicles per year (average for 41 years) distributed according to vehicle weight

Weight (tonf)	Number of vehicles	Weight (tonf)	Number of vehicles
<10	290,888	60 - 70	13375
10 - 20	228628	70 - 80	8961
20 - 30	161258	80 - 90	4314
30 - 40	110581	90 - 100	1892
40 - 50	73377	100 - 110	498
50 - 60	32756	110 - 120	133

4. METHODOLOGY

The focus of the assessment is on two suspected factors considered most relevant to the incident's failure, namely failure due to overstress and fatigue-related failure. For the possibility of overstress, strength examination is carried out in accordance with Indonesian codes (SNI), taking into account the load specified by the code and also accounting for the actual load during the collapse incident. For the possibility of fatigue, an examination is conducted based on the AASHTO LRFD 2012 [23] procedure, and the fatigue load is derived from Weigh-in-Motion (WIM). The methodology for the strength check is outlined in the following section, followed by an explanation of the fatigue assessment.

4.1 Bridge Strength Analysis

The Cincin Lama Bridge was modeled using Midas Civil software [25]. In this study, only the superstructure of the fourth span of the bridge, which collapsed, with a length of 50.29 m, was modeled and analyzed because the substructure was still in good condition. The 3D model of the bridge includes a steel main truss, floor plates, stringers, cross girders, and wind bracing. Fig.6 illustrates the bridge model. The analysis was conducted considering only gravitational loads, in accordance with the collapse event dominated by gravitational loading.

4.1.1 Investigation criteria

According to [9] and [10], incorrect assumption of loads is one of the frequent causes of bridge collapse. To address this concern, a process involves reviewing the actual loads the bridge is likely to encounter throughout its operational lifespan and comparing them to the initially assumed loads during the design phase. In this regard, strength checks are conducted against three load criteria, as follows:

1. In accordance with the criteria of the design code when the bridge was built, SNI 03-1725-1989 [26], to assess the compliance of the bridge to the applicable regulations at the time of its construction. Note that SNI 03-1725-1989 is a design code that formalizes the design guidelines used since 1970 in Indonesia.
2. In accordance with the current design code in Indonesia, SNI 1725-2016 [22], to determine the strength of the bridge based on the current design criteria. Since the construction of the bridge, the design code has been upgraded several times. Research has been done to improve the live load specification in the code [27].
3. Based on the estimated loads that occurred shortly before the bridge collapsed (actual load).

This investigation is crucial for uncovering the collapse's immediate cause and guiding future infrastructure improvements for similar structures' safety and reliability.

4.1.2 Bridge Load According to Indonesian Code

According to the Indonesian code, a bridge's load consists of permanent, traffic, and environmental loads. For this assessment, we are considering the permanent load and traffic load only. The permanent load includes the structural self-weight (SW) and the superimposed dead load (SDL), which are calculated based on the material unit weight, as outlined in Table 5. Traffic loads are modeled as lane load "D", which is formed by a combination of uniformly distributed load (UDL) and knife-edge load (KEL). The bridge traffic load, as per SNI 1725-2016 [22], is presented in Table 6.

Table 5 Bridge material unit weight

Material	Unit weight (kN/m^3)
steel	78.75
concrete	25.00
asphalt	22.00

Table 6 Bridge traffic load (SNI 1725-2016 [22])

Lane load	Span length	Intensity
UDL	$L \leq 30$ m	9.0 kPa
	$L > 30$ m	9.0(0.5 + 15/L) kPa
KEL		49 kN/m

There are several differences in the loading criteria between SNI 03-1725-1989 [26] and SNI 1725-2016 [22], mainly in the increase of live load criteria as follows:

1. Increase of Lane Load "D" for uniformly distributed load (UDL) from q = 6.52 kN/m^2 to 7.184 kN/m^2.

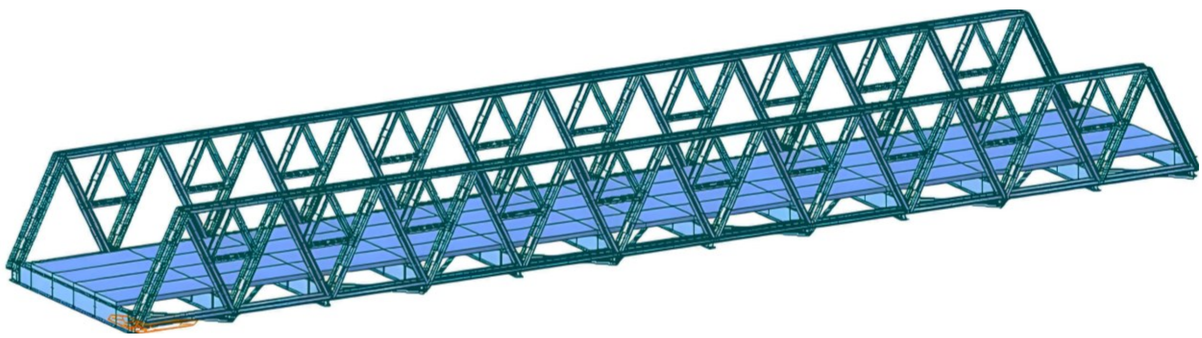

Fig.6 The 3D model of The Cincin Lama Bridge typical steel span

2. Increase of Lane Load "D" for knife edge load (KEL) from P = 42.8 kN/m to 49.0 kN/m and with dynamic factor, the load increased by 30%.
3. Increase of Truck Load “T” for design truck load from 45 tons to 50 tons and dynamic load factor allowance.

4.1.3 LRFD factors

In the analysis based on design codes, the LRFD method is employed, incorporating load factors and resistance reduction factors in accordance with the referenced codes. The load and resistance factors specified in SNI 03-1725-1989 [26] and SNI 1725-2016 [22] codes are detailed in Table 7 and Table 8, respectively. Notably, there is an increase in the load factors in the newer code. For the examination involving actual loads, a load factor of 1.0 is applied to all load conditions, accompanied by a strength reduction factor of 0.9. This reduction factor is set at 0.9 because material strength and condition testing were not conducted at the time of the incident, thereby neglecting the potential influence of corrosion or other usage defects.

Table 7 Load combinations and load factors according to SNI 03-1725-1989 and SNI 1725-2016 codes

SNI 03-1725-1989						
Load comb.	SW	SDL	Lane Load	Brake	Ped.	Wind
Str. I	1.25	1.25	-	-	-	1.25
Str. II	1.40	1.40	1.40	1.40	11.40	1.40
Str. III	1.50	1.50	-	-	-	-
Str. IV	1.50	1.50	1.50	-	-	-
SNI 1725-2016						
Load comb.	SW	SDL	Lane Load	Brake	Ped.	Wind
Str. I	1.1	2.0	1.8	1.8	1.8	-
Str. IIa	1.1	2.0	1.4	1.4	1.4	-
Str. IIb	1.1	2.0	-	1.4	1.4	-
Str. III	1.1	2.0	-	-	-	1.4

Table 8 Strength reduction factors for the bridge strength analysis

Strength Analysis	Strength reduction factor	
	SNI 1989 and SNI 2016	Actual Load
Compression	0.85	0.9
Tension yield	0.90	0.9
Tension fracture	0.75	0.9
Bolt	0.75	0.9

4.1.4 Strength Check of The Main Truss

The initial step in the strength analysis involves calculating the maximum internal forces in each member while accounting for moving traffic loads. To accurately consider the critical traffic load position and distribution, influence line diagrams were generated for each member. Subsequently, the critical position and distribution of both the traffic lane load and the actual loads for each member were determined by referencing the influence line diagrams.

The strength assessment of the main truss members and connections aligns with the criteria outlined in the design code. In particular, for the strength check of the upper chord compression bars, it is essential to establish the out-of-plane buckling length of the truss prior to conducting the strength assessment. To derive the equivalent buckling length, a linear buckling analysis was performed on the bridge model. The resulting equivalent buckling length is then applied in the relevant code equation.

4.1.5 Transverse Girders and Stringers

The transverse girders and stringers are analyzed through composite section analysis due to the contribution of the concrete floor slab to the strength of the transverse girders and stringers.

4.2 Evaluation of Fatigue

The fatigue evaluation refers to the fatigue evaluation method in AASHTO LRFD 2012 [23]. The method used to evaluate fatigue is through the *S-N* curve based on the Palmgren-Miner rule. The law of damage accumulation is expressed in Eq. (2).

$$D=\Sigma\frac{n_i}{N_i} \quad (2)$$

where D denotes the cumulative damage, N_i is the fatigue life under constant amplitude loading with amplitude S_i and n_i is the number of load cycles at this amplitude.

According to the AASHTO LRFD 2012 standards, the Cincin Lama Bridge is categorized as D detailing, signifying a vulnerability to potential cracks in the bolt-hole regions due to stress concentration. This category aligns with a constant amplitude fatigue threshold (CAFT) value of 48.26 MPa. Additionally, a dynamic load allowance (IM) of 15% is incorporated into the truck/bus load to accommodate fatigue and fracture limits.

Expanding on the insights from [28], it has been established that evaluating the fatigue life of the bridge necessitates considering the dynamic effects of vehicles. To integrate this dynamic consideration, the fatigue loads outlined in Table 4 are multiplied by the dynamic load allowance and applied at critical locations as per the influence line previously developed for strength analysis. This approach is used for determining the stress amplitude. The stress amplitudes are then categorized into ranges, and the frequency of occurrence for each stress amplitude range is tallied based on vehicle frequency.

The elements most susceptible to fatigue are those experiencing the highest cyclic tensile stress. An assessment of these critical elements involves evaluating their accumulated damage according to Eq. (2), considering the number of cycles per year within each stress amplitude range derived from the analyzed Weigh-in-Motion (WIM) data.

5. RESULTS AND DISCUSSION

The results of the assessment, conducted following the methodology outlined in the previous section, are summarized in this section. It begins with the outcomes of the strength examination and proceeds with the results of the fatigue assessment.

5.1 Strength Check Analysis Results

As a tool to determine the location and distribution of the most critical loads, both for strength checks and fatigue analysis, influence lines have been developed for each element in the main truss. Fig.7 illustrates three samples of the generated influence lines.

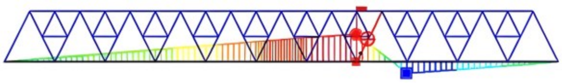

(a)

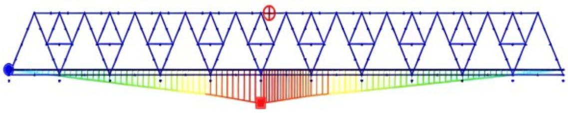

(b)

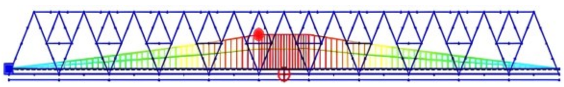

(c)

Fig.7 Influence line diagrams for (a) a diagonal element, (b) a top chord element, and (c) a bottom chord element

To assess the strength of compression members, particularly the upper chord, a linear buckling analysis was conducted on the bridge model. The analysis revealed that the equivalent buckling length is 0.4 times the span length. The most critical buckling mode is illustrated in Fig.8.

The strength analysis results for elements experiencing the highest internal forces are displayed in Table 9, presenting stress ratios for various element types and load combinations. Table 10 showcases the strength examination outcomes for elements and connections near the supports, where the collapse was initiated.

From the strength examination results, it is evident that the structure meets the strength requirements based on the SNI 03-1725-1989 code [26], but it is unable to meet the more stringent requirements of the 2016 regulations. It is also apparent that the estimated actual loads have a smaller influence compared to the SNI 1725-2016 code [22]. However, the stress ratio resulting from the actual loads has exceeded the requirements as well. Similar observations are seen in the analysis of elements and connections in the vicinity of the collapse area. Interestingly, it is shown here that the stress ratio in the collapse area is indeed higher than the stress ratio in the center of the span. This is because the forces in the center of the span are indeed greater, but this is compensated by using larger cross-sectional elements. Thus, the critical area is indeed in the elements near the supports where the collapse occurred.

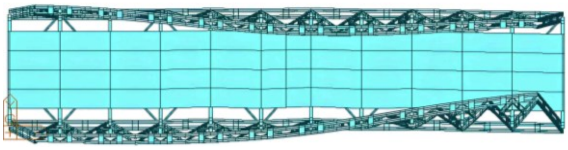

Fig.8 Plan view of out-of-plane buckling mode of the bridge

Table 9 The critical stress ratio for members experiencing the maximum internal forces.

Element	Stress Ratio		
	SNI 1989	SNI 2016	Actual
Brace (tension)	0.41	0.72	0.68
Brace (compression)	0.36	0.51	0.40
Bottom chord	0.46	1.00	0.72
Top chord	0.81	1.41	1.11
Trv. Beam Moment	0.46	0.84	1.30
Trv. Beam Shear	0.45	0.83	0.89
Stringer Moment	0.34	0.64	1.20
Stringer Shear	0.14	0.21	0.41

Table 10 The critical stress ratio for members and connections in the area where the collapse initiated

Element	Stress Ratio		
	SNI 1989	SNI 2016	Actual
Brace (tension)	0.63	1.07	0.77
Brace (compression)	0.35	0.60	0.49
Bottom chord	0.87	1.49	1.20
Gusset plate	0.66	1.10	0.96
Bolt	0.85	1.40	1.01

5.2 Fatigue Analysis Results

To implement the Palmgren-Miner rule, the distribution of stress amplitude ranges (S) has been calculated, as explained in Section 4.2. The results are compiled and presented in Table 11. The damage accumulation is computed by applying Eq. (2) to the data in Table 11. To illustrate the damage accumulation calculation, Fig.9 shows a histogram depicting stress amplitude ranges (*S*) against the number of cycles (*n*). This histogram is then compared with the *S-N* curve, following the AASHTO 2012 [23] code.

Upon analyzing the calculation results, it was determined that the cumulative fatigue damage resulting from one year of traffic loading on the Cincin Lama Bridge, as inferred from the Weigh-in-Motion (WIM) measurements, amounted to 0.0253. Consequently, the projected fatigue life of the bridge is approximately 39.5 years. Notably, this figure falls slightly below the bridge's age at the time of collapse, which was 41 years. This indicates that the bridge's structural integrity might have been compromised, leading to its untimely failure.

Table 11 Number of cycles per year (average for 41 years) distributed according to stress magnitude

Stress (*S*) (MPa)	Number of cycles (*n*)	Percentages
<10	257,667	27.81
10 - 20	207,853	22.43
20 - 30	175,462	18.93
30 - 40	107,395	11.59
40 – 50	81,674	8.81
50 - 60	54,328	5.86
60 - 70	26,450	2.85
70 - 80	8,861	0.96
80 - 90	5,078	0.55
90 - 100	1,560	0.17
100 - 110	265	0.03
110 – 120	66	0.01

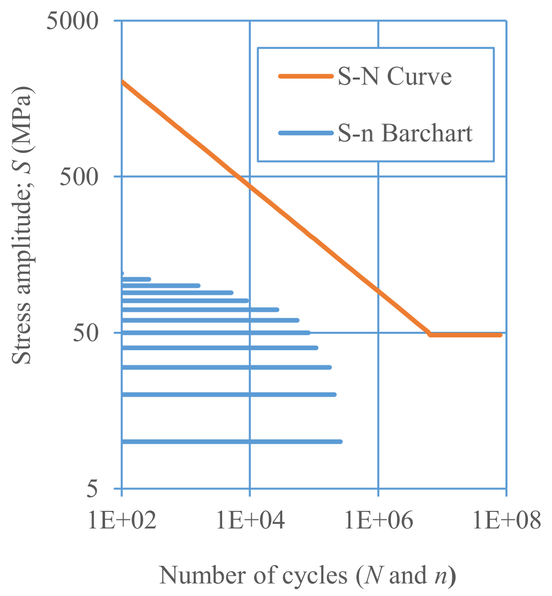

Fig.9 Stress and number of cycles (*S-n*) plot and comparison to *S-N* curve

6. CONCLUSIONS

Based on the analysis conducted, the following conclusions can be drawn:

1. Based on the structural analysis of the bridge, it can be inferred that the Cincin Lama Bridge was constructed in compliance with the applicable design code at that time.
2. According to the strength analysis, it was found that the Cincin Lama Bridge 4th Span, which experienced collapse, did not meet the requirements for design gravity load based on the current design code.
3. The strength analysis revealed that the bridge does not meet the criteria for supporting the estimated actual gravity load. According to the current regulations, the stress ratio observed is still lower than that caused by the design load. The calculations indicate that the most critical area indeed lies in the region where the collapse occurred.
4. From the fatigue evaluation results using Weigh in Motion (WIM) measurements and applying the S-N curve and Miner's equation, it was determined that the fatigue life of the bridge is 39.5 years, while the bridge collapsed at the age of 41 years. This suggests that fatigue cracks in the bridge were highly likely to have occurred prior to its collapse.

7. REFERENCES

[1] Bhattacharya, S., Tokimatsu, K., Goda, K., Sarkar, R., Shadlou, M., and Rouholamin, M., Collapse of Showa Bridge During 1964 Niigata Earthquake: A quantitative Reappraisal on the Failure Mechanisms, Soil Dynamics and Earthquake Engineering, Vol. 65, Issue 1, 2014, pp. 55-71.

[2] Deng, L., Wang, W., and Yu, Y., State-of-the-Art Review on the Causes and Mechanisms of Bridge Collapse, J. Perform. Constr. Facil. Vol. 30, Issue 2, 2016, pp. 04015005:1- 04015005:13.

[3] Furukawa, A., and Kawamatsu, Y., Earthquake Damage Assessment for RC Piers By Time-Frequency Analysis Considering Entire Bridge, GEOMATE Journal, Vo. 25, Issue 111, 2023, pp. 1–8.

[4] Hashimoto, S., Abe, M., and Fujino, Y., Damage Analysis of Hanshin Expressway Viaducts during 1995 Kobe Earthquake. III: Three-Span Continuous Girder Bridges, J. Bridge Eng., Vol. 10, Issue 1, 2005, pp. 61-68.

[5] Hsu, Y. T., and Fu, Ch. C., Study of Damaged Wushi Bridge in Taiwan Earthquake, Practice Periodical on Structural Design and Construction, Vol. 5, Issue 4, 2000, pp. 166-171.

[6] Schexnayder, C., Alarcón, L. F., Antillo, E. D., Morales, B. C., and Lopez, M., Observations on

Bridge Performance during the Chilean Earthquake of 2010, J. Constr. Eng. Management, Vol. 140, Issue 4, 2014, pp. B4013001:1-B4013001:6
[7] Sun, Z., Wang, D. Guo, X. Si, B. and Huo, Y., Lessons Learned from the Damaged Huilan Interchange in the 2008 Wenchuan Earthquake, J. Bridge Eng., Vol. 17, Issue 1, 2012, pp. 15-24.
[8] Aggarwal, V., and Parameswaran, L., Effect of Overweight Trucks on Fatigue Damage of a Bridge, In: Matsagar, V. (ed.), Advances in Structural Engineering 2015, Springer, India 2015, pp 2483-2491.
[9] Biezma, M. V., and Schanack, F., Collapse of Steel Bridges, J. Perform. Constr. Facil., ASCE, Vol. 21, Issue 5, 2007, pp. 398–405.
[10] Wardhana, K. and Hadipriono, F. C., Analysis of Recent Bridge Failures in the United States, J. Performance of Constructed Facilities, Vol. 17, Issue 3, 2003, pp. 144-150.
[11] Astaneh-Asl, A., Progressive Collapse of Steel Truss Bridges, the Case of I-35W Collapse, In Proc. 7th Int. Conf. on Steel Bridges, Guimaraes, Portugal, 2008, Invited keynote, pp. 1-10.
[12] Lora, M. A. R., Study of the I-35 W Bridge Collapse Mechanism, Thesis Master of Science in Civil Engineering, Virginia Polytechnic Institute and State University, 2013, pp. 1-90.
[13] Kawai, Y., Siringoringo, D., and Fujino, Y., Failure Analysis of the Hanger Clamps of the Kutai-Kartanegara Bridge from Fracture Mechanics Viewpoint, J. of JSCE, Vol. 2, Issue 1, 2014, pp. 1-6.
[14] Imran, I., Santoso, B., Pramudito, A., and Zamad, M. K., Simulation of Palu IV Bridge Collapse using Near-Fault Ground Motions, In Proc. IABSE Congress – The Evolving Metropolis, New York City, 2019, pp. 1314-1320.
[15] Directorate General of Highways, Standard Drawings of Road and Bridge Works, Vol. 2, No. 04/BM/2005, Ministry of Public Works, Jakarta, 2005, pp. 52-128.
[16] Directorate General of Highways, Handling & Maintenance of Callender Hamilton (CH) Bridges, No. 013/BM/2008, Ministry of Public Works, Jakarta, 2008, pp. 1-138.
[17] Cantero, D., and Gonzales A., Bridge Damage Detection Using Weigh-in-Motion Technology, J. Bridge Engineering, ASCE, Vol. 20, Issue 5, 2015, pp. 1-10.
[18] Iatsko, O., Babu, A. R., Stallin, J. M., and Nowak, A. S, Weigh-in-Motion Based Fatigue Damage Assessment, Transportation Research Record: J. the Transportation Research Board, Vol. 2674, Issue 8, 2020, pp. 710-719.
[19] Liu, Y., Zhang, D., Li., Z., Zhang, H. and Jiang, N., Fatigue Load Model Using the Weigh-in-Motion System for Highway Bridges in China, J. Bridge Engineering, ASCE, Vol. 22, Issue 6, 2017, pp.1-8.
[20] Jang, B. and Jamshid, M., Significance of Fatigue Damage from Overload Trucks on Bridge Load Rating, MATEC Web of Conferences, Vol. 165, Issue 5, 2018, pp. 1-6.
[21] Nugraha, W., Evaluasi Umur Fatik Elemen Baja Jembatan Standar Tipe Komposit Menggunakan Data WIM. Jurnal Jalan Jembatan, Vol. 34, Issue 1, 2017, pp. 21-33.
[22] SNI 1725-2016, Loading for Bridges, National Standardization Agency, 2016, Jakarta, pp. 1-67.
[23] AASHTO LRFD, Bridge Design Specifications, 6th Ed., AASHTO (American Association of State Highway and Transportation Officials), 2012, Washington DC, USA, pp. 1:1-15:14.
[24] Directorate General of Highways, Pavement Design Manual (revised 2017), Circular Letter of Director General of Highways No: 04/SE/Db/2017, Ministry of Public Works and Housing, Jakarta, 2017, pp. 1-235.
[25] Midas Software, Analysis for Civil Structures, Midas Civil, Korea, 2019, pp. 1-383.
[26] SNI 03-1725-1989, Highway Bridge Loading and Design Guidelines, National Standardization Agency, 1989, Jakarta, pp. 1-24.
[27] Nugraha, W., Sidi, I. D., Suarjana, M., and Zulkifli, E., Reliability Evaluation of Steel Truss Bridge due to Traffic Load Based on Bridge Weigh-In-Motion Measurement, Structural Monitoring and Maintenance, Vol. 9, Issue 4, 2022, pp. 323–336.
[28] Wang, W., Lu, D., and Xudong, S., Fatigue Design of Steel Bridges Considering the Effect of Dynamic Vehicle Loading and Overloaded Trucks, Journal Bridge Engineering, ASCE, Vol. 21, Issue 9, 2016, pp. 1-12.

Copyright © Int. J. of GEOMATE All rights reserved, including making copies, unless permission is obtained from the copyright proprietors.